THE JOURNAL OF PHYSICAL CHEMISTRY A

Article

Cite This: J. Phys. Chem. A 2018, 122, 8762−8775

pubs.acs.org/JPCA

Conformation-Specific Spectroscopy of Asparagine-Containing Peptides: Influence of Single and Adjacent Asn Residues on Inherent Conformational Preferences

Karl N. Blodgett,[†] Joshua L. Fischer,[†] Jaeyeon Lee,[‡] Soo Hyuk Choi,[‡] and Timothy S. Zwier*[,†]

[†]Department of Chemistry, Purdue University, West Lafayette, Indiana 47907-2084, United States

[‡]Department of Chemistry, Yonsei University, Seoul 03722, Korea

Supporting Information

ABSTRACT: The infrared and ultraviolet spectra of a series of capped asparagine-containing peptides, Ac-Asn-NHBn, Ac-Ala-Asn-NHBn, and Ac-Asn-Asn-NHBn, have been recorded under jet-cooled conditions in the gas phase in order to probe the influence of the Asn residue, with its $-CH_2-C(=O)-NH_2$ side chain, on the local conformational preferences of a peptide backbone. The double-resonance methods of resonant ion-dip infrared (RIDIR) spectroscopy and infrared−ultraviolet hole-burning (IR−UV HB) spectroscopy were used to record single-conformation spectra in the infrared and ultraviolet, respectively, free from interference from other conformations present in the molecular beam. Ac-Asn-NHBn spreads its population over two conformations, both of which are stabilized by a pair of H-bonds that form a bridge between the Asn carboxamide group and the NH and C=O groups on the peptide backbone. In one the peptide backbone engages in a 7-membered H-bonded ring (labeled $C7_{eq}$), thereby forming an inverse γ-turn, stabilized by a C6/C7 Asn bridge. In the other the Asn carboxamide group forms a C8/C7 H-bonded bridge with the carboxamide group facing in the opposite direction across an extended peptide backbone involving a C5 interaction. Both Ac-Ala-Asn-NHBn and Ac-Asn-Asn-NHBn are found exclusively in a single conformation in which the peptide backbone engages in a type I β-turn with its C10 H-bond. The Asn residue(s) stabilize this β-turn via C6 H-bond(s) between the carboxamide C=O group and the same residue's amide NH. These structures are closely analogous to the corresponding structures in Gln-containing peptides studied previously [Walsh, P. S. et al. *PCCP* **2016**, *18*, 11306−11322; Walsh, P. S. et al. *Angew. Chem. Int. Ed.* **2016**, *55*, 14618−14622], indicating that the Asn and Gln side chains can each configure so as to stabilize the same backbone conformations. Spectroscopic and computational evidence suggest that glutamine is more predisposed than asparagine to β-turn formation via unusually strong side-chain−backbone hydrogen-bond formation. Further spectral and structural similarities and differences due to the side-chain length difference of these similar amino acids are presented and discussed.

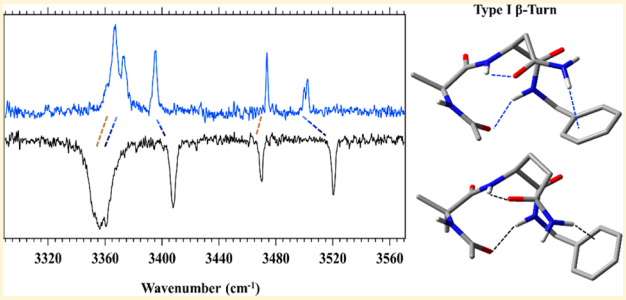

1. INTRODUCTION

The polar amino acids asparagine and glutamine, differing by one methylene group, are the only two naturally occurring amino acids that contain carboxamide groups in their flexible side chains. Both amino acids are heavily involved in neurodegenerative disease pathogenesis.[1−5] At the genetic level, CAG codon repeat disorders result in long tracts of glutamine residue repeats within proteins, which subsequently fold into β-sheet oligomers that aggregate to form insoluble amyloid fibrils, the hallmark of neurodegenerative disease.[6,7] Nine late-onset neurodegenerative diseases, including Huntington's disease, are attributed to polyglutamine expansions.[8,9]

Prion diseases, on the other hand, are characterized by the misfolding of native proteins into self-aggregating β-sheet units which ultimately form insoluble amyloid fibrils that wreak havoc on the central nervous system.[10,11] The so-called prion-forming domains of the proteins, which are responsible for protein misfolding, are rich in both asparagine (Asn, N) and glutamine (Gln, Q).[12−14] In humans, prion diseases are caused by the misfolding of the PrP^C protein into its prion form, PrP^{Sc}.[15] These diseases include Creutzfeldt−Jakob disease, fatal familial disease, and Gerstmann−Straussler−Scheinker syndrome.[15,16] Rather than being propagated through the genome, prion forms of misfolded proteins induce other normally folded proteins to isomerize to the prion state, thereby causing a chain reaction of protein misfolding and disease propagation.

These amyloid fibrils all appear to contain a common structural motif: the steric zipper. In this structure at least two β-sheets are interdigitated with one another, oftentimes sterically locking in asparagine and glutamine residues.[2,17,18] Studies using solid-state NMR spectroscopy, X-ray crystallog-

Received: August 29, 2018
Revised: October 16, 2018
Published: October 21, 2018

DOI: 10.1021/acs.jpca.8b08418
J. Phys. Chem. A 2018, 122, 8762−8775

raphy, and EPR spectroscopy have demonstrated that many amyloids formed from prion and prion-like proteins fold into an in-register parallel β-sheet in which steric zipper monomer units hydrogen bond with one another to form parallel β-sheets which propagate along the fibril axis. These proteins include β-amyloid (Alzheimers)[19−21] and the yeast proteins Sup35[22,23] and Ure2p.[24−26] Many studies have sought to determine the role of Asn and Gln in the prion-forming domains of proteins as well as the difference in aggregation propensity between the residues.[1−3,10,14,27−31] In this study we are interested in determining the role that Asn plays in local protein conformation by spectroscopically characterizing the conformational impact of the alkyl-linked carboxamide side chain in three increasingly complex peptides.

To this end, we use a bottom-up approach toward understanding nature's preference for asparagine in neurodegenerative diseases. We seek to determine the role that one or two Asn residues has on the intrinsic folding propensities of three short, capped peptides: Ac-Asn-NHBn, Ac-Ala-Asn-NHBn, and Ac-Asn-Asn-NHBn (Figure 1). Each peptide is

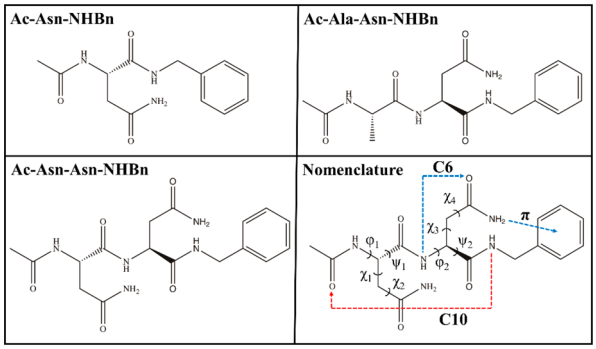

Figure 1. Chemical structures of the molecules studied in this work along with the definition of important dihedral angles used herein. Note that hydrogen bonds designated in blue indicate backbone−side-chain hydrogen bonding, while those designated in red indicate backbone−backbone hydrogen bonding.

capped with a benzyl group which acts as a UV chromophore. We characterize the inherent conformational preferences of each peptide in the absence of environmental perturbations by recording spectra of the gas-phase molecules in a molecular beam using mass-resolved double-resonance infrared and ultraviolet spectroscopy. Computational and experimental studies on close analogues of Ac-Asn-NHBn show extended and inverse γ-turn backbone structures to be among the lowest energy conformational isomers (conformers).[32,33] Previous conformational studies in our group on analogous glutamine-containing peptides showed that Ac-Gln-NHBn had population spread out between three conformers in the molecular beam: an extended backbone structure, an inverse γ-turn backbone structure, and a turned backbone structure lacking any backbone−backbone amide hydrogen bonds.[34] Mons and co-workers identified three conformers of Ac-Phe-Asn-NH_2 in a molecular beam: a β-turn, a γ-turn, and an extended backbone structure.[33] The analogous Gln-containing dipeptides each funneled all of the population into a single conformer: the type I β-turn.[34,35]

Comparing the conformational preferences of Asn with those of the analogous Gln-containing peptides gives direct insight into the impact of the shortening of the carboxamide side chain by a single methylene group. Armed with the conformer-specific spectra and assignments, we thus address the similarities and differences of the Asn and Gln conformations.

Studies of synthetic foldamers containing β-residues are particularly relevant to the hydrogen-bonding motifs accessible to the Asn side-chain amide group. The elongated peptide backbones in β-peptides give access to hydrogen-bonding cycles not available to α-peptides.[36−39] The Asn residues are capable of forming the same hydrogen bonds by virtue of them having the same number of carbon atoms (two) between backbone and side-chain amide groups as separate residues in the peptide backbone of β-peptides. On this basis, it is fair to anticipate similar hydrogen bonding in the Asn-containing peptides to that observed in the β-peptides. As we shall see, the Asn-containing peptides presented in Figure 1 are capable of forming hydrogen bonds which support extended peptide backbones, inverse γ-turns, and type I β-turns.

2. METHODS

2.1. Experimental Methods. A detailed description of the synthetic procedure for each molecule studied herein can be found in the Supporting Information. The experimental procedure for studying their spectroscopy has been described in detail elsewhere.[40,41] Briefly, sublimation of the sample was achieved by nonresonant laser desorption.[42,43] The crystal sample was crushed into a fine powder and rubbed onto the surface of a sanded graphite rod, which is coupled into the vacuum chamber via a load lock assembly. The fundamental of a Nd:YAG (20 Hz, Continuum minilite II, 5 mJ/pulse, 2 mm beam diameter) laser is absorbed at the surface of the graphite rod, imparting energy to desorb the neutral sample into the gas phase. The rod is kept directly under the 1000 μm diameter orifice of a pulsed valve (Parker, series 9) which introduces short bursts of high-pressure argon backing gas (20 Hz, ~5.5 bar backing pressure, 500 μs) into the vacuum chamber. The sample is entrained in the supersonic expansion and is subsequently cooled into the zero-point vibrational levels of low-energy conformational minima. A linear actuator (NSC 200, Newport) slowly pushes the sample-containing rod into the chamber, thereby ensuring consistent sample concentration in each desorption laser pulse. The supersonic expansion passes through a conical skimmer, becoming a molecular beam, which then travels into the ion source region of a Wiley−McLaren time-of-flight (TOF) mass spectrometer. The cold, neutral molecules are then characterized using a suite of laser-based methods.

The first step in characterizing each molecule is using one-color resonant two-photon ionization (R2PI) in which a UV spectrum with contributions from all conformations with measurable population is obtained. The doubled output of a Nd:YAG pumped tunable dye laser is scanned across the benzyl UV chromophore absorption region (37 500−37 820 cm^{-1}). When the frequency is resonant with a vibronic transition of a cold conformer a photon is absorbed, immediately after which a second ionizing photon is absorbed. Monitoring the parent mass channel of the absorbing species as a function of UV frequency allows the recording of the electronic spectrum. Conformer-specific infrared spectra are recorded using resonant ion-dip infrared spectroscopy (RIDIRS). In this scheme the UV laser (20 Hz) is fixed on a vibronic transition belonging to one of the conformers in the R2PI spectrum, thereby generating a constant ion signal that is proportional to the ground state population of that conformer.

DOI: 10.1021/acs.jpca.8b08418
J. Phys. Chem. A 2018, 122, 8762−8775

The tunable output of a KTP/KTA-based optical parametric converter (LaserVision, 10 Hz) spatially overlaps and temporally precedes by 200 ns the UV beam. As the IR laser is scanned across the regions of interest, resonance between the IR frequency and a ground state vibration of the conformer being probed results in the removal of a fraction of ground state population and a subsequent dip in ion signal. A gated integrator (Stanford Research Systems, SR 250) in active baseline subtraction mode outputs the difference in integrated parent ion signal as a function of IR frequency, resulting in a conformer-specific infrared spectrum. Infrared−ultraviolet (IR−UV) hole burning is used to generate conformer-specific UV spectra. This scheme is identical to RIDIRS except that the IR laser is fixed on a conformer-specific vibrational transition while the UV laser is scanned.

2.2. Computational Methods. The potential energy surface of each molecule studied herein was initially explored with an exhaustive force field search using a torsional-sampling Monte Carlo Multiple Minimum conformational search within the MacroModel computational suite. Searches were performed with both the OPLS3 and the Amber* force fields until successive search iterations yielded no additional structures. A redundant conformer elimination performed on the pool of structures calculated to be below 50 kJ/mol generated from both force fields yielded starting structures for higher level calculation.

Density functional theory geometry optimization and harmonic vibrational frequency calculations were carried out on each candidate structure using the Gaussian09 computational package[44] with Becke's B3LYP hybrid functional supplemented with the D3 version of Grimme's dispersion correction[45] and Becke−Johnson damping[46] (GD3BJ). This modified hybrid functional was used in conjunction with the 6-31+G(d) Pople basis set. Tight convergence and an ultrafine grid were implemented in each calculation to ensure output of the best possible normal-mode frequencies to compare with experiment. Harmonic vibrational frequencies were calculated for all structures. Scale factors of 0.958, 0.981, and 0.970 were used in the hydride stretch, amide I, and amide II regions, respectively, to account for anharmonicity of the vibrations. Energy considerations, vibronic assignments, and agreement between calculated and experimental IR frequencies led to the conformational assignment of each experimentally observed conformer.

2.3. Nomenclature. Hydrogen bonds are designated with the C*n* notation, in which *n* is the number of atoms involved in a hydrogen-bonded cycle. We invoke the same conformational labeling scheme used in previous studies of analogous Gln-containing peptides.[34,35] Hydrogen bonds are listed in the following stylized order: backbone−backbone//*side-chain−backbone*//**side-chain−side-chain**. For example, the labeled conformer in Figure 1 is designated as a C10//*C6/π* hydrogen-bonded structure where a 10-membered hydrogen-bond ring is formed between backbone amide groups while the N-terminal Asn carboxamide group acts as a bridge to the peptide backbone (or in this case, cap) comprised of *C6* and NH···π H bonds. In addition, and unless otherwise stated, backbone−backbone hydrogen bonds are shown as blue dashed lines in the figures, while *side-chain−backbone* hydrogen bonds are designated with red dashed lines.

In certain parts of the discussion, both 'Asn' and 'N' will be used to designate asparagine while both 'Gln' and 'Q' will be used to designate glutamine. Important peptide backbone and side-chain dihedral angles are defined in Figure 1. Additional dihedral angles, designated as χ_{Q1} and χ_{Q2}, refer to the one additional N- and C-terminal Gln side-chain dihedrals, respectively. Finally, the '*i*+' notation will be used to identify groups within particular residues along the peptide backbone. The *C6* of the labeled molecule in Figure 1, for example, is between the amide NH and the Asn C═O of residue *i*+2, while the C10 is between the amide NH of residue *i*+3 and the C═O of residue *i*. Crystal structures referenced within were taken from the RCSB Protein Data Bank[47] after a secondary structure search using the Motivated Proteins web tool.[48]

3. RESULTS AND ANALYSIS

3.1. Ac-Asn-NHBn—Infrared Spectroscopy and Conformational Assignment. R2PI and IR−UV hole-burning spectra revealed two unique conformers of Ac-Asn-NHBn present in the molecular beam (Figure S1). The RIDIR spectra of conformer A and conformer B are presented in the top (red) and bottom (blue) portions of Figure 2, respectively. Below

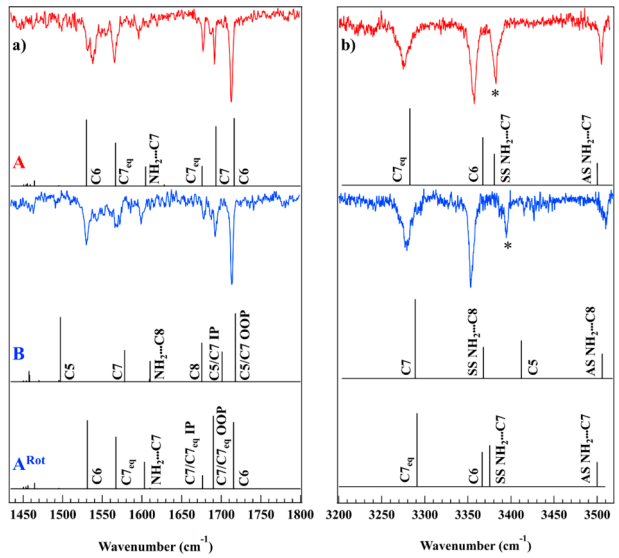

Figure 2. RIDIR spectra of the two conformers of Ac-Asn-NHBn, conformer A (red trace) and conformer B (blue trace), in the hydride stretch (b) and amide I/II (a) regions. Stick spectra presented below each experimental trace represent the scaled, harmonic vibrational frequencies of each assigned conformer calculated at the B3LYP-D3BJ/6-31+G(d) level of theory and labeled with the main carrier(s) of the vibration. Transitions marked with an asterisk are those used to collect IR−UV hole-burning spectra. See text for further discussion.

each experimental trace is a stick spectrum that depicts the scaled, harmonic vibrational frequencies of each best-fit structure. Each transition is labeled with the main carrier(s) of the vibration as determined through inspection of the best-fit structure. The RIDIR spectra of conformers A and B are very similar to one another; however, small wavenumber shifts are present, confirming that two unique conformers are present.

Given the two backbone amide NH groups and the NH_2 group on the Asn side chain, we anticipate observing four NH stretch fundamentals for each conformer, as observed in Figure 2b. In the hydride stretch region both conformers have their highest frequency transition well below ∼3560 cm^{-1}, the frequency at which the asymmetric (AS) stretch of a free NH_2 group appears. This indicates that both conformers have their

DOI: 10.1021/acs.jpca.8b08418
J. Phys. Chem. A 2018, 122, 8762−8775

Asn NH_2 group involved in a hydrogen bond. The highest frequency transitions of conformer A and B appear at 3505 and 3510 cm^{-1}, respectively. The RIDIR spectrum of conformer B has asymmetrically broadened peaks that are likely due to a small spectral contamination from the RIDIR spectrum of conformer A. It is likely that the UV absorption of conformer A begins in the region where conformer B absorbs. However, this is difficult to determine via the IR−UV hole-burning spectra of conformer A due primarily to the low signal and shot-to-shot fluctuations inherent to laser desorption. The fact that in both conformers the two highest frequency hydride stretches occur at wavenumbers in which the other conformer has zero absorption provides evidence that although qualitatively similar, the sources of these IR spectra are indeed independent of one another.

On the basis of agreement between experiment and theory and as can be seen in Figure 3, conformer A is assigned to a

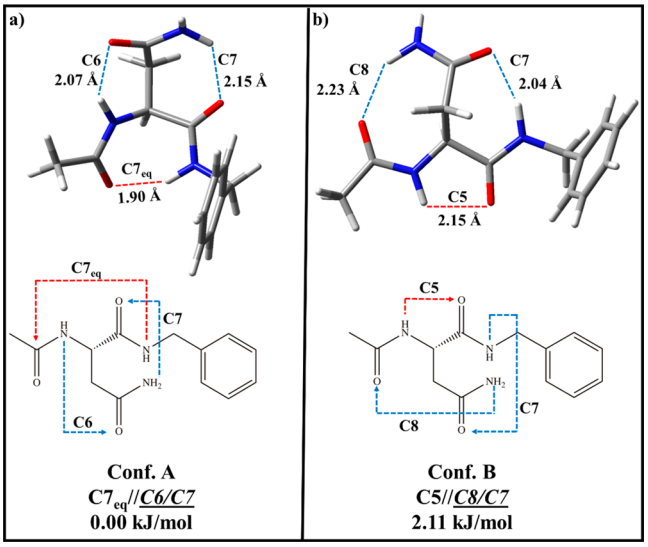

Figure 3. Assigned structure of (a) conformer A and (b) conformer B of Ac-Asn-NHBn; 3D structure and 2D hydrogen-bonding schematic are presented for each conformer, as well as the hydrogen-bonding designation and relative zero-point-corrected potential energies.

$C7_{eq}$//C6/C7 structure with a bridged side-chain−backbone hydrogen-bonding motif and the backbone in an inverse γ-turn. This conformer was calculated to be the global energy minimum. Table 1 presents hydrogen-bond distances and experimental vibrational frequencies for the Asn-containing peptides studied herein and analogous Gln-containing peptides,[34,35] while Table S1 presents an extended version of Table 1 which includes other β-amino acid-containing foldamers studied previously.[36−38]

Conformer A has three additional hydride stretch fundamentals at 3383, 3357, and 3275 cm^{-1}. The transition at 3383 cm^{-1} is assigned to the symmetric NH_2 stretch of the Asn moiety, forming a pair with the asymmetric NH_2 stretch at 3505 cm^{-1}. Analysis of the assigned structure of conformer A shows that this NH_2 group is involved in a C7 hydrogen bond with the C-terminal carbonyl group. The vibrational splitting[49] between the coupled asymmetric and symmetric NH_2 stretches is thus 122 cm^{-1}, a relatively small value which makes sense in light of the nonoptimum hydrogen-bond distance (2.15 Å) and angle of approach (129.3°). As a result, throughout this work we will use asymmetric and symmetric stretch (AS and SS)

Table 1. Hydrogen-Bonding Cycles, Calculated Distances, and Experimental Vibrational Frequencies for Those Interactions Found in the Asn-Containing Peptides Studied in This Work Compared with the Analogous Gln-Containing Peptides Studied Previously

molecule	H-bond cycle	H-bond distance (Å)	experimental frequency (cm^{-1})
Ac-Asn-NHBn			
Conf A ($C7_{eq}$//C6/C7)	$C7_{eq}$	1.90	3275
	C6	2.07	3357
	C7	2.15	3383 (3505)
Conf B (C5//C8/C7)	C5	2.15	3394
	C8	2.23	3353 (3510)
	C7	2.04	3279
Conf A^{Rot} ($C7_{eq}$//C6/C7)	$C7_{eq}$	1.91	3279
	C6	2.09	3353
	C7	2.13	3394 (3310)
Ac-Gln-NHBn[a]			
Conf A (C5//C8)	C5	2.11	3402
	C8	1.96	3310
Conf B (C7/π)	C7	1.97	3354
	π		3415 (3529)
Conf C ($C7_{eq}$//C7/C8/π)	$C7_{eq}$	1.92	3270
	C7	1.99	3343
	C8	2.24	3400 (3509)
Ac-Ala-Asn-NHBn			
Conf A (C10//C6/π)	C10	1.99	3367
	C6	2.08	3373
	π		3395 (3502)
Ac-Ala-Gln-NHBn[a]			
Conf A (C10//C7/π)	C10	2.02	3357
	C7	1.97	3361
	π		3408 (3520)
Ac-Asn-Asn-NHBn			
Conf A (C10//C6/C6/π)	C10	2.01	3350
	C6	2.16	3383
	C6	2.07	3359
	π		3393 (3505)
Ac-Gln-Gln-NHBn[b]			
Conf A (C10//C7/C7/π)	C10	1.99	3345
	C7	1.91	3324
	C7	1.98	3360
	π		3409 (3521)

[a]From ref 34. [b]From ref 35.

designations to describe the vibrations of the NH_2 moiety, as the normal-mode analysis of the NH_2 vibrations shows large contributions from each NH oscillator in the coupled vibrations, even when one NH is involved in a hydrogen bond and the other is more or less free. The band at 3357 cm^{-1} is localized on the N-terminal NH group which is involved in a C6 hydrogen bond with the O=C oxygen on the Asn side chain. The lowest frequency hydride stretch at 3275 cm^{-1} has a fwhm of ~17 cm^{-1}, which is indicative of strong coupling to background states associated with a strong hydrogen bond. This transition is assigned to the C-terminal NH oscillator involved in a $C7_{eq}$ hydrogen bond with the N-terminal O=C.

DOI: 10.1021/acs.jpca.8b08418
J. Phys. Chem. A 2018, 122, 8762−8775

This strong hydrogen bond has a calculated NH···O=C distance of 1.90 Å and NHO angle of approach equal to 151°.

The amide I region of conformer A (Figure 2) contains vibrational transitions which report on the hydrogen bonds from the perspective of the C=O hydrogen-bond acceptor oscillators. Conformer A has three C=O stretch fundamentals appearing at 1713, 1691, and 1677 cm^{-1}, which are assigned to the localized stretch fundamentals of the C=O oscillators involved in the C6, C7, and $C7_{eq}$ hydrogen bonds, respectively. While the amide I (and amide II) region is less physically intuitive to analyze, C=O stretch fundamentals are generally shifted down in frequency when accepting hydrogen bonds, with further down shifts arising when the coamide NH acts as hydrogen-bond donor.[42,50] The $C7_{eq}$ C=O stretch is the most down shifted in frequency, affirming the strong nature of this hydrogen bond.

The amide II region of conformer A, contributed to primarily by the NH bending motion, shows three clear transitions with increasing intensity at 1596, 1565, and 1538 cm^{-1}. The match between the experimental and the calculated frequencies allows us to assign the peak at 1596 cm^{-1} to the Asn NH_2, which acts as C7 hydrogen-bond donor. The peaks at 1565 and 1538 cm^{-1} are assigned to the hydrogen-bond-donating groups of the $C7_{eq}$ and C6 cycles, respectively. The integrated intensity of the C6 cycle at 1538 cm^{-1} is the largest of the amide II transitions. This intensity gain has been theoretically characterized as cooperative coupling between the dipole derivatives induced by the amide II nuclear motion and the electronic charge flux through the O···H interaction.[51−54] In the case of C5 and C6 hydrogen bonds, these two dipole derivative vectors are nearly parallel to one another, resulting in an enhancement of the transition intensity.

Conformer B has its hydride stretch fundamentals at 3510, 3394, 3353, and 3279 cm^{-1}. The highest frequency transition is readily assigned to the asymmetric NH_2 stretch, leaving the peaks at 3394 and 3353 cm^{-1} as possibilities for the symmetric stretch transition with vibrational splittings of 115 or 157 cm^{-1}, respectively. Since the asymmetric stretch is shifted down in frequency by ∼50 cm^{-1} from where the unperturbed vibration occurs at 3562 cm^{-1}, one would anticipate the symmetric stretch to be shifted by more than 115 cm^{-1}. On that basis, the transition at 3353 cm^{-1} is tentatively assigned to the symmetric NH_2 fundamental.

Two possible assignments are presented in Figure 2 for conformer B. The assignment we deem to be most consistent with experiment is labeled as B in the figure and is due to the conformer shown in Figure 3b, a C5//C8/C7 structure in which the Asn amide group forms C8 and C7 H-bonds with the amide groups on either side. In this assignment the transition at 3353 cm^{-1} is ascribed to the symmetric NH_2 fundamental involved in a C8 hydrogen bond with the N-terminal C=O group. Likewise, the transition at 3394 cm^{-1} is assigned to a C5 hydrogen bond between the Asn backbone amide group components. The shift down in frequency of the C5 hydrogen-bonded NH, which can appear as high as ∼3440 cm^{-1}, may be attributed to cooperative effects from the nearest-neighbor hydrogen-bonded interactions (see section 4.1 for further discussion). The broad (15 cm^{-1} fwhm) transition at 3279 cm^{-1} is assigned to a C7 hydrogen bond between the C-terminal NH and Asn C=O. This strong hydrogen bond has a calculated NH···O distance of 2.04 Å and angle of approach of 160°.

The tentative assignment of conformer B to the C5//C8/C7 structure shown in Figure 3b has its energy just 2.11 kJ/mol above that of conformer A, the global minimum. The amide I spectra of conformer B show three clearly resolved transitions at 1713, 1692, and 1678 cm^{-1} in order of decreasing intensity. The transitions at 1713 and 1692 cm^{-1} are assigned to the out-of-phase and in-phase combinations, respectively, of the carbonyl groups in the C5 and C7 cycles. The small transition at 1678 cm^{-1} is assigned to the N-terminal C=O in the C8 cycle.

The three amide II transitions appear at 1599, 1569, and 1529 cm^{-1}. The weak transition at 1599 cm^{-1} is assigned to the NH_2 group involved in the C8 cycle, while the transition at 1569 cm^{-1} is attributed to the C7 bound NH. The intense peak at 1529 cm^{-1} is assigned to the extended backbone C5 hydrogen bond. As discussed above, the large intensity of this transition is likely due to the interaction of the transition dipole caused by the NH bending motion and the electronic charge flux through the O···H interaction. This interaction geometry is optimized in the C5 hydrogen bond, in which both vectors are nearly parallel to one another.

The stick diagram A^{Rot} in Figure 2 presents an alternative possibility for conformer B, a benzyl rotamer of the assigned conformer A inverse γ-turn structure, with structure shown in Figure S2. This conformer is calculated to be the second lowest energy structure at 1.7 kJ/mol above the global minimum (conformer A). As can be seen in Figure 2, the simulated spectra also fit well with the experimental IR spectra of conformer B. While the currently assigned extended structure fits better with the experimental data in the hydride stretch region, the calculated spectra of A^{Rot} fits somewhat better in the amide I and II regions.

The ambiguity of the assignment of conformer B hinges upon whether population is kinetically trapped in the laser desorption/supersonic expansion process. Figures S2 and S3 show a structural comparison of conformer A and conformer A^{Rot} and the relaxed potential energy scan about the relevant dihedral of conformer A, respectively. Since the barrier to relaxation of A^{Rot} to A is modest (5 kJ/mol), one would anticipate cooling of population from A^{Rot} to A. However, since the energy difference between the minima is also small, we cannot definitively eliminate the possibility that the transitions of conformer B are due to A^{Rot}. In what follows the tentative assignment of conformer B as the C5//C8/C7 extended backbone structure will be used to guide the discussion, with the understanding that this assignment is tentative.

3.2. Ac-Ala-Asn-NHBn—Infrared Spectroscopy and Conformational Assignment. R2PI and IR−UV hole-burning spectra proved the presence of one major conformer of Ac-Ala-Asn-NHBn present in the molecular beam (Figure S4). The RIDIR spectra of Ac-Ala-Asn-NHBn in the hydride stretch and amide I/II regions are presented in Figure 4a and 4b, respectively. The hydride stretch region shows five well-resolved peaks appearing at 3502, 3474, 3395, 3373, and 3367 cm^{-1}, as anticipated based on the structure (Figure 1). Given the absence of competing high-frequency transitions, the band at 3502 cm^{-1} can be tentatively assigned to the asymmetric stretch of the Asn NH_2 group, which based on its shift away from the free transition frequency is in a hydrogen bond. This leads us to assign the transition at 3474 cm^{-1} to a free amide NH stretch. The three remaining transitions all fall between 3360 and 3400 cm^{-1}, a region which has been demonstrated in

DOI: 10.1021/acs.jpca.8b08418
J. Phys. Chem. A 2018, 122, 8762−8775

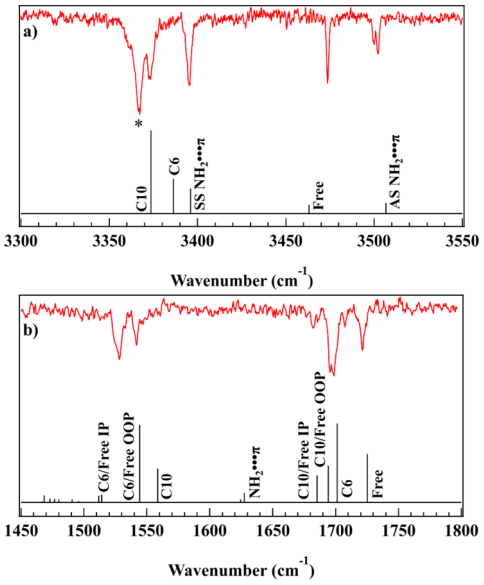

Figure 4. RIDIR spectra of the assigned conformer of Ac-Ala-Asn-NHBn in the (a) hydride stretch and (b) amide I/II regions. Black stick spectra represent the scaled, harmonic, normal-mode frequencies of the assigned structure calculated the B3LYP-D3BJ/6-31+G(d) level of theory. Labels indicate the main carrier(s) of the vibration.

previous studies to contain transitions arising from C6, C7, and C10 hydrogen bonds.[34−38,55,56] Consistent with these qualitative deductions, the agreement of the experimental spectrum with the calculated spectrum presented in Figure 4 leads to assignment of the sole conformer of Ac-Ala-Asn-NHBn to a C10//*C6/π* structure, which was calculated to be the global energy minimum. As can be seen from the assigned structure in Figure 5, the NH_2 asymmetric stretch frequency is shifted down in frequency due to an $NH_2\cdots\pi$ interaction.

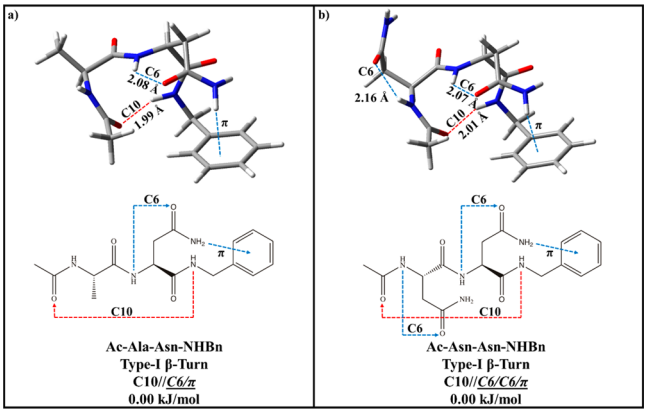

Figure 5. Assigned structures of (a) Ac-Ala-Asn-NHBn and (b) Ac-Asn-Asn-NHBn; 3D structure and 2D hydrogen-bonding schematic are presented for each conformer, as well as the hydrogen-bonding designation and relative zero-point corrected potential energies (among each molecule).

With the assigned structure in hand, the remaining hydride stretch transitions are readily assigned. The 3395 cm^{-1} transition arises from the symmetric NH_2 stretch, while the 3373 cm^{-1} is assigned to the *C6* cycle comprised of the Asn amide NH and Asn side-chain C═O. The lowest frequency transition at 3367 cm^{-1} arises from the NH group engaged in a C10 hydrogen bond between the C-terminal NH and the N-terminal C═O. This strong hydrogen bond has an NH···O═C distance of 1.99 Å and angle of approach equal to 157°. This C10 hydrogen bond between the C═O of residue *i* and the NH of residue *i*+3 is structurally characteristic of a *β*-turn. Indeed, inspection of the backbone dihedral angles of residue *i* +1 and *i*+2 results in the categorization of this conformer to a type I *β*-turn structure. As we shall discuss, this structural motif is the same as that formed by the analogous glutamine-containing peptide.[34]

The amide I region consists of an isolated transition at 1721 cm^{-1}, a split peak with closely spaced maxima at 1699 and 1695 cm^{-1}, and a weak transition at 1682 cm^{-1}. The high-frequency peak is assigned to the free Ala amide C═O oscillator. The most intense amide I transition at 1699 cm^{-1} is assigned to the Asn side-chain C═O involved in the *C6* hydrogen bond. The 1695 cm^{-1} transition is assigned to the out-of-phase combination of the C10 and N-terminal free C═O groups, with the in-phase combination appearing at 1682 cm^{-1}. The discrepancy between calculated and experimental intensities of these modes is likely due to the out-of-phase transition mixing and borrowing intensity from the near-resonant *C6* transition.

The amide II spectrum shows two clear transitions at 1542 and 1528 cm^{-1}, with the two weak transitions at lower frequency predicted by the best-fit structure likely lost in the experimental noise. Regardless, the experimental frequency position and intensity pattern compared with that of the assigned structure give further confidence in the assignment. The experimentally observed transition at 1542 cm^{-1} is assigned to the C10 NH wagging motion, while the transition at 1528 cm^{-1} is attributed to the out-of-phase NH bend combination of the *C6* and free N-terminal NH groups.

3.3. Ac-Asn-Asn-NHBn—Infrared Spectroscopy and Conformational Assignment. R2PI and IR−UV hole-burning spectra determined that the population of Ac-Asn-Asn-NHBn resides in a single conformation in the molecular beam (Figure S5). The RIDIR spectra of Ac-Asn-Asn-NHBn in the hydride stretch and amide I/II regions are shown as the top and bottom traces of Figure 6, respectively. Cursory comparison of the hydride stretch spectrum of Ac-Ala-Asn-NHBn with that of Ac-Asn-Asn-NHBn shows qualitative similarities in frequency and intensity patterns (Figures S6 and S7). Of course, with the additional Asn functional group, the hydride stretch region shown in Figure 6 contains two additional transitions due to the coupled stretches of the N-terminal Asn NH_2 group. The two highest frequency stretches at 3543 and 3505 cm^{-1} are readily assigned to the asymmetric stretches of a free and hydrogen-bound NH_2 group, respectively. The known coupling strength between the two NH bonds of the carboxamide group allows the transition at 3430 cm^{-1} to be confidently assigned to the symmetric stretch of the free NH_2. Given the similar frequencies of the hydrogen-bound asymmetric NH_2 stretches in Ac-Ala-Asn-NHBn and Ac-Asn-Asn-NHBn, the band at 3396 cm^{-1} is tentatively assigned to the symmetric stretch of the hydrogen-bound NH_2 group.

Comparison of the best-fit calculated frequencies with experimental frequencies lead to assignment of the sole conformer of Ac-Asn-Asn-NHBn to a C10//*C6/C6/π* structure, which is calculated to be the global minimum energy conformer among the pool of competing structures. On the basis of this assignment, the band at 3386 cm^{-1} arises from

DOI: 10.1021/acs.jpca.8b08418
J. Phys. Chem. A 2018, 122, 8762−8775

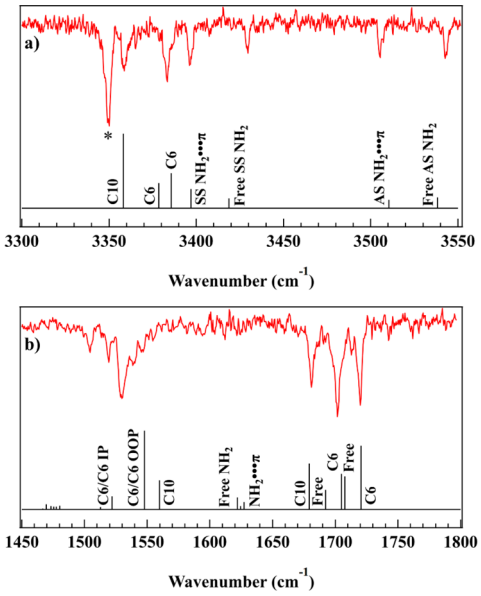

Figure 6. RIDIR spectra of the single observed conformer of Ac-Asn-Asn-NHBn in the hydride stretch (top) and amide I/II (bottom) regions. Black stick spectra display the scaled, harmonic, normal-mode frequencies of the assigned structure calculated the B3LYP-D3BJ/6-31+G(d) level of theory. Labels indicate the main carrier(s) of the vibration.

a *C6* hydrogen bond between the N-terminal amide NH and Asn C═O, while the transition at 3359 cm^{-1} is due to the analogous C-terminal *C6* hydrogen bond. This is the same hydrogen bond in Ac-Ala-Asn-NHBn that appears at 3373 cm^{-1} (Figure S7). The intense low-frequency transition at 3350 cm^{-1} is assigned to a C10 hydrogen bond between the NHBn NH and the acyl C═O. This large hydrogen-bonded cycle has a NH···O═C distance of 2.01 Å and angle of approach equal to 158°, properties very similar to the analogous C10 H bond in Ac-Ala-Asn-NHBn. Indeed, the dihedral angles between residue *i*+1 and residue *i*+2 of this conformer also classify it as a type I β-turn former. Interestingly, the analogous Gln-containing dipeptide also forms a type I β-turn under isolated, jet-cooled conditions,[35] a point to which we will return later.

The excellent fit of the spectrum calculated for the assigned conformer with experiment enables a ready analysis of the amide I and II regions of the spectrum. The highest frequency transition at 1720 cm^{-1} is assigned to the Asn C═O involved in a *C6* hydrogen bond with the N-terminal amide NH. The most intense peak in the amide I region has two closely spaced maxima at 1702 and 1701 cm^{-1}. The spectral overlap of these peaks results in each transition lending intensity to and borrowing intensity from one another. They are assigned to the free N-terminal amide C═O and the C-terminal Asn C═O, which is involved in a *C6* H bond with its amide NH. A small maximum at 1691 cm^{-1} mostly lost in the noise, sandwiched between two much larger transitions, is tentatively assigned to the C-terminal free C═O oscillator, while the final amide I peak at 1681 is due to the N-terminal C═O involved in the cross-molecule C10 hydrogen bond.

The spectrum in the amide II region is less well resolved and hence serves more to confirm the assignment than as a diagnostic tool. The assigned conformer has two low-intensity peaks around 1625 cm^{-1}, which are not readily observed in the experimental spectrum. The transition at 1640 cm^{-1} is assigned to the bending motion of the C-terminal NH involved in the

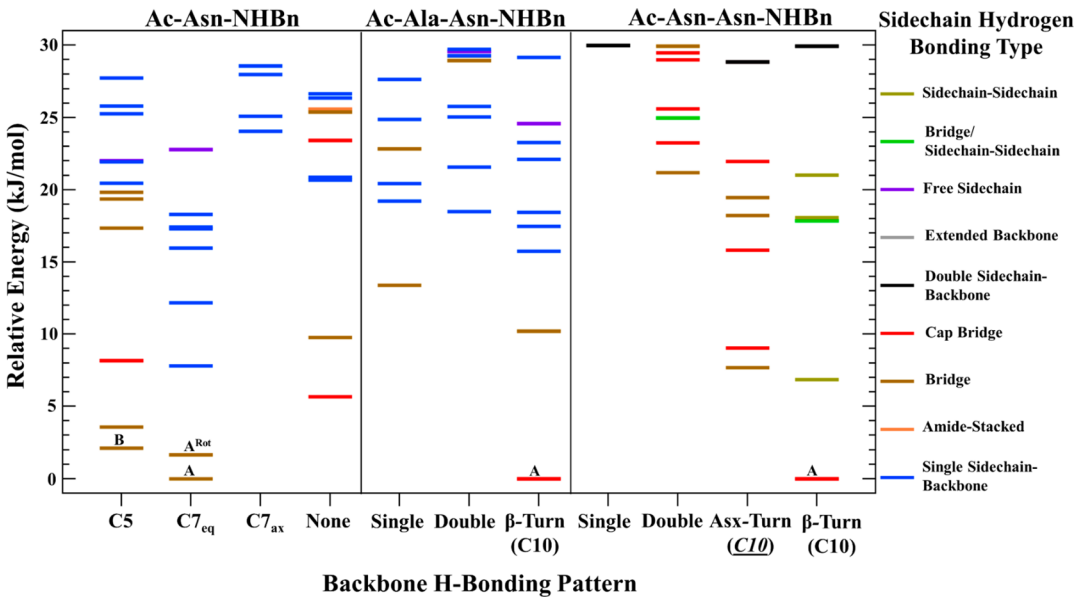

Figure 7. Energy level diagrams for the three asparagine-containing molecules studied herein. Each conformer has its relative zero-point-corrected energy (B3LYP-D3BJ/6-31+G(d)) plotted as a function of backbone hydrogen-bonding pattern with the following stylized nomenclature: backbone−backbone//*side-chain−backbone*//**side-chain-side-chain**. Asx-Turns are structures where a *C10* hydrogen bond is formed between the carboxamide C═O of an Asn on residue *i* and the backbone NH of residue *i*+2. Each conformer energy level is also color coded to further indicate the type(s) of hydrogen bond(s) in which the amide side chain(s) is (are) involved. Experimentally observed conformers are labeled with their letter designation. "Bridge" designates structures where both the hydrogen-bond donor and acceptor on the same carboxamide side chain are involved in hydrogen bonds to the backbone or backbone and cap (Cap Bridge). Double Side chain-Backbone designates structures in Ac-Asn-Asn-NHBn where each amide side chain is involved in a single hydrogen bond to the backbone. Side chain-Side chain designates structures in Ac-Asn-Asn-NHBn where the two carboxamide side chains are hydrogen bonding with each other.

DOI: 10.1021/acs.jpca.8b08418
J. Phys. Chem. A 2018, 122, 8762−8775

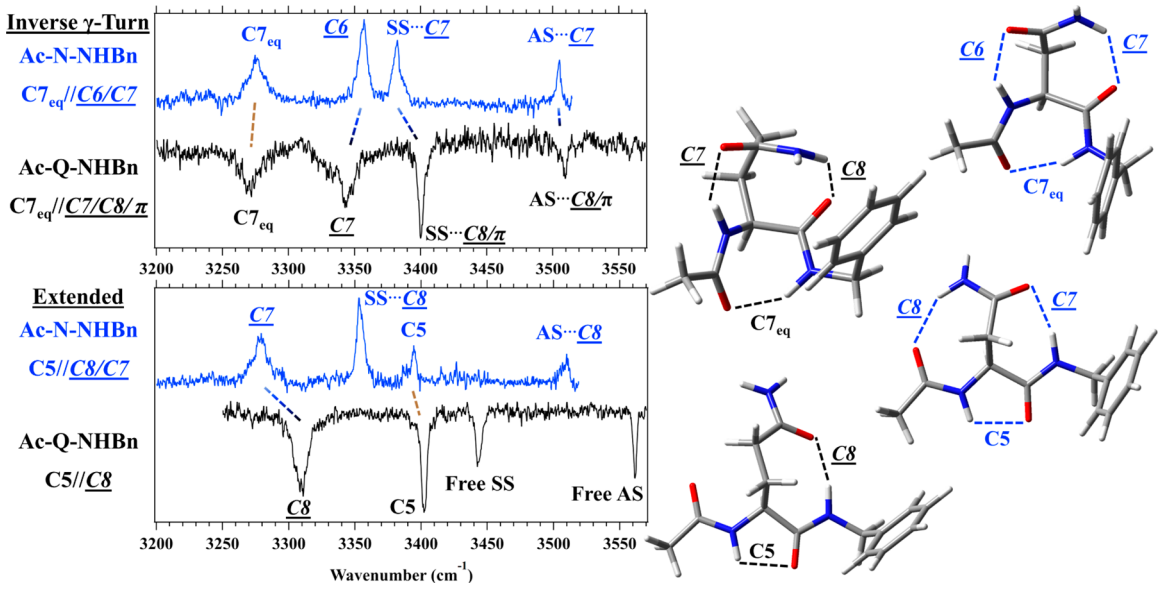

Figure 8. Hydride stretch IR spectra and experimentally assigned structures of analogous Ac-Asn-NHBn and Ac-Gln-NHBn conformers. Asn hydrogen bonds and spectra are designated in blue, while those of Gln are designated in black. Transitions are labeled with the main carrier of the vibration with analogous hydrogen bonds in Asn and Gln analogs connected with dashed lines and color coded in the following way: the same hydrogen-bonded cycles connected with brown lines and analogous (Cn − (Cn + 1)) cycles with faded blue to black lines.

Table 2. Calculated Dihedral Angles (in degrees) of the Asn(N)-Containing Peptides Studied in This Work and the Analogous Gln(Q)-Containing Peptides[a]

	residue (i+1)					residue (i+2)				
structure	φ_1	ψ_1	χ_1	χ_2	χ_{Q1}	φ_2	ψ_2	χ_3	χ_4	χ_{Q2}
inverse γ-turn										
Ac-N-NHBn conf A ($C7_{eq}$//C6/C7)	−82	63	50 (g^+)	103						
Ac-N-NHBn conf A^{Rot} ($C7_{eq}$//C6/C7)	−82	56	51 (g^+)	100						
Ac-Q-NHBn conf C ($C7_{eq}$//C7/C8/π)[b]	−82	56	74 (g^+)	−40 (g^-)	110					
inverse γ-turn canonical value[c]	−75	65								
extended backbone										
Ac-N-NHBn conf B (C5//C8/C7)	−169	−178	−137 (a)	91						
Ac-Q-NHBn conf A (C5//C8)[b]	−162	169	−103 (a)	−64 (g^-)	167					
extended backbone canonical value	180	180								
type I β-turn										
Ac-A-N-NHBn (C10//C6/π)	−68	−13				−80	0	62 (g^+)	102	
Ac-A-Q-NHBn (C10//C7/π)[b]	−70	−13				−73	−11	83 (g^+)	−61 (g^-)	151
A-N crystal structure avg[d]	−63	−26				−92	8			
type I β-turn canonical value[e]	−60	−30				−90	0			
Ac-N-N-NHBn (C10//C6/C6/π)	−76	1	61 (g^+)	104		−83	−3	62 (g^+)	105	
Ac-Q-Q-NHBn (C10//C7/C7/π)[f]	−73	−8	68 (g^+)	−87 (g^-)	−165	−71	−13	84 (g^+)	−62 (g^-)	150
N-N crystal structure avg[g]	−62	−25				−96	4			

[a]Also listed are either the canonical dihedral angles or the average values of those extracted from the Protein Data Bank.[47] [b]From ref 34. [c]From ref 57. [d]SI Table 9 [e]From ref 58. [f]From ref 35. [g]SI Table 8.

C10 hydrogen bond. The two transitions at 1530 and 1519 cm^{-1} form the out-of-phase and in-phase combinations, respectively, of the two C6 hydrogen-bonded amide NH groups with some C10 NH bend mixed in.

4. DISCUSSION

Conformer-specific infrared spectra in the hydride stretch and amide I/II regions have been used in conjunction with calculated vibrational frequencies to assign the four conformers spanning the three Asn-containing peptides investigated in this study. In each case the assigned conformers belong to the lowest energy conformational families calculated at the B3LYP-D3BJ/6-31+G(d) level of theory. Agreement between experimental and theoretical vibrational frequencies, when combined with the fact that the structures are among the calculated energetic minima, gives confidence that the assigned structures accurately reflect the inherent conformational preferences of the cold, gas-phase molecules studied herein.

In order to understand the broader conformational landscape for these Asn-containing peptides, Figure 7 presents an energy diagram that displays the full set of conformers with calculated energies within 30 kJ/mol of the global minimum of the three Asn-containing peptides. In the diagrams we have partitioned the conformers horizontally into distinct peptide backbone H-bonding patterns and further color coded each

DOI: 10.1021/acs.jpca.8b08418
J. Phys. Chem. A 2018, 122, 8762−8775

energy level to indicate the hydrogen-bonding type for the Asn side chain. Upon inspection of the energy diagram, it is immediately clear that the number of conformational families made available by the Asn residue increases in complexity with both the length of the peptide backbone and the number of Asn residues. The three types of structures experimentally observed represent two different canonical turn types (inverse γ, type I β-turn) and an extended structure, all of which occur regularly in proteins.

The two assigned bridged structures of Ac-Asn-NHBn energetically compete with one another and are representative of the only two conformational families under 5 kJ/mol. While both conformers have bridged side-chain−backbone interactions, the NH_2 groups engage in hydrogen bonds with C═O groups at different positions along the peptide backbone. In the extended structure the carboxamide NH_2 is interacting with the N-terminal C═O while the analogous amido group in the inverse γ-turn structure is interacting with the C-terminal C═O. By forming these bridge structures with the carboxamide side chain, the structure also incorporates the maximum number of hydrogen bonds for each molecule.

The two capped dipeptides funnel all population into a type I β-turn peptide backbone, with a strong energetic preference relative to all competitors. Indeed, in Ac-Ala-Asn-NHBn and Ac-Asn-Asn-NHBn the observed type I β-turn is more stable than any other in the conformational pool by 10 and 7 kJ/mol, respectively.

With firm conformational assignments of the present Asn-containing peptides and their analogous Gln-containing peptides from previous studies by our group, we are now in a position to investigate the impact that the difference in side-chain length between Asn and Gln (which differ by a single methylene group) has on peptide structure and stability as made manifest by the experimental vibrational spectra and best-fit structures. In what follows we focus on each structure type in turn, with emphasis placed on the structural and spectral similarities and differences between analogous Asn and Gln peptides.

4.1. Inverse γ-Turns. Conformer A of Ac-Asn-NHBn, with its $C7_{eq}$//C6/C7 hydrogen-bonding architecture, forms an inverse γ-turn at the shortest chain length possible. Conformer C of Ac-Gln-NHBn also forms an inverse γ-turn, with analogous $C7_{eq}$//C7/C8/π hydrogen bonds.[34] Figure 8 compares the structures and spectra of the Asn- and Gln-stabilized γ-turns, and Table 2 lists the corresponding dihedral angles. In what follows the Asn γ-turn will be referred to simply as γN and the Gln γ-turn as γQ. In both structures the carboxamide side chains form hydrogen-bonded bridges with the peptide backbone, resulting in //C6/C7 and //C7/C8/π side-chain−backbone motifs in Asn and Gln, respectively, with very similar φ/ψ backbone dihedrals (Table 2).

The difference of one methylene group between the carboxamide side-chains of γN and γQ dictates that the side-chain χ dihedrals will be different from one another. Indeed, the Gln carboxamide group bends back over the γ-turned backbone and engages in a dispersive π interaction with the benzyl cap, an additional interaction for which Asn lacks the required flexibility. The NH_2 AS fundamental is higher in frequency in γQ than γN by only 4 cm^{-1}, even though the C7 is ∼0.1 Å shorter in γN than the C8 in γQ. In this case, it is the additional π interaction in γQ which serves to shift down in frequency the AS NH_2 to within 4 cm^{-1} of the γN C7.

The $C7_{eq}$ backbone H bond is extraordinarily strong in both γN (1.90 Å, 3275 cm^{-1}) and γQ (1.92 Å, 3270 cm^{-1}). These two hydrogen bonds are among the strongest $C7_{eq}$ hydrogen bonds observed, shifting down in frequency by as much as 100 cm^{-1} from a $C7_{eq}$ observed previously (see Table 1).[59,60] James et al. observed, in their study of mixed α/β synthetic foldamers, that NH groups belonging to amides whose components act as both hydrogen-bond donor and acceptor have NH bond lengths longer than NH groups on amides that are not involved in such cooperative interactions.[38] This is explained by the notion that, during hydrogen bonding, electron density is transferred from the electron-rich C═O to the antibonding orbital of NH with the nuance that this electron transfer appears to involve electron donors and acceptors on the *same* amide group, which cannot be directly hydrogen bonded with one another. This description offers an appealing physical explanation for the large $C7_{eq}$ frequency shifts in γN and γQ: In both structures the bridging carboxamide group closes a triple-hydrogen-bonding cycle in which all three present amide groups are maximally involved in hydrogen bonding. The NH and C═O along the peptide backbones not involved in the $C7_{eq}$, which if not for the carboxamide-containing side chains would be free, are both involved in hydrogen bonding, resulting in a large net cooperative strengthening effect. This cooperative strengthening likely contributes to the large shift down in frequency of the $C7_{eq}$ in both γN and γQ. The N-terminal bridge component in γN is a C6 hydrogen bond with a distance of 2.07 Å and angle of approach equal to 137°. The analogous γQ C7 measures 1.99 Å with an angle of approach equal to 150°. As expected based on these metrics, the C7 NH stretch is shifted down in frequency to the C6 by 14 cm^{-1}.

On the basis of a search of the Protein Data Bank, Milner-White concluded that compound inverse γ-turns, γ_n with n = 2−5, occur regularly within β-sheet strands.[57] These γ-turn repeat segments take the form of ribbons with a slight right-handed twist, a structure the author referred to as a 2.2_7-helix. Given that proteinaceous β-sheets also twist in the right-handed direction, Milner-White postulated that compound inverse γ-turns could play a role in the local stabilization of β-strands en route to β-sheet formation. This proposition is especially intriguing in light of the high concentration of Asn and Gln residues in β-sheet-rich amyloid fibrils as well as the uniquely and unusually strong $C7_{eq}$ hydrogen bonds formed in both γN and γQ. Gas-phase tests of the 2.2_7-helicity of poly-N and poly-Q would be worthwhile in pursuit of testing Milner-White's proposition as it is applied to nature's preference for Asn and Gln in prion-forming domains.

To test the influence that the bulky aromatic NHBn cap has on preferred structures, geometry optimization and energy calculations were carried out on the 35 low-energy (<30 kJ/mol) Ac-N-NHBn structures plotted in Figure 7, with the NHBn cap substituted with an NHMe cap (Table S5). Six unique structural families within 10 kJ/mol in the NHBn cap group reduce to only two unique structural families within 15 kJ/mol of the global energy minimum: with the NHMe cap present $C7_{eq}$//C6/C7 (0.00 kJ/mol) and C5//C8/C7 (1.97 kJ/mol), the two families to which conformer A and conformer B, respectively, belong. This indicates that the two conformations observed in the case of Ac-Asn-NHBn are indeed the preferred structures, regardless of C-terminal cap.

As an additional check on the robustness of these conformational preferences to temperature changes, free

DOI: 10.1021/acs.jpca.8b08418
J. Phys. Chem. A 2018, 122, 8762−8775

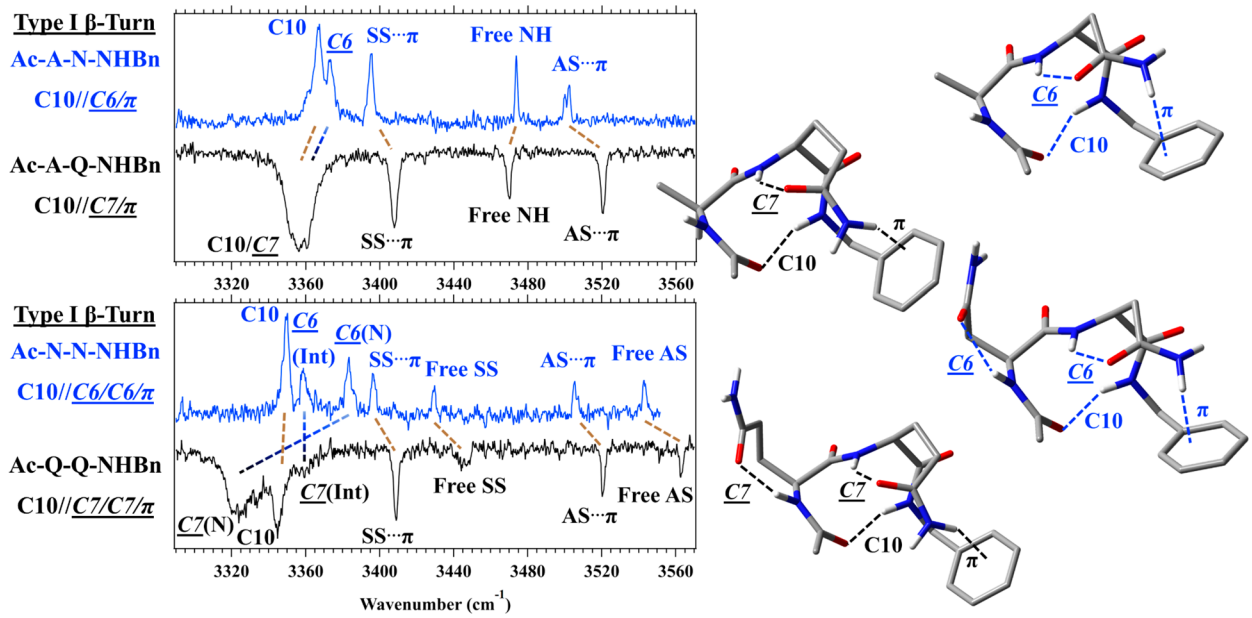

Figure 9. Hydride stretch IR spectra and experimentally assigned structures of analogous Ac-Ala-Asn-NHBn and Ac-Ala-Gln-NHBn (top) and Ac-Asn-Asn-NHBn and Ac-Gln-Gln-NHBn (bottom) conformers. Asn hydrogen bonds and spectra are designated in blue, while those of Gln are designated in black. Transitions are labeled with the main carrier of the vibration with analogous hydrogen bonds going from Asn to Gln connected with dashed lines and color coded in the following way: the same hydrogen-bonded cycles connected with brown lines and analogous (Cn − (Cn + 1)) cycles with faded blue to black lines.

energy corrections calculated at room temperature were carried out to determine whether entropic forces result in preferred structures different from those observed in the molecular beam (Table S2). Even when ranked in relative free energy, γN remains the energetic minimum, suggesting that this local conformation may play an important role in environments in which free energy, rather than internal energy, dictates conformation.

4.2. Extended Structures. Conformer B of Ac-Asn-NHBn has a C5//C8/C7 extended backbone architecture with near planar backbone φ/ψ dihedral angles of −169° and −178°. Conformer A of Ac-Gln-NHBn also forms an extended backbone structure, comprised of a C5//C8 hydrogen-bonding pattern and similar φ/ψ backbone dihedral angles of −162° and 169° (Table 2). Henceforth, the extended structures of Ac-Asn-NHBn and Ac-Gln-NHBn will be referred to as eN and eQ, respectively. The lower half of Figure 8 displays a comparison between the structures and the hydride stretch spectra of eN and eQ. While both structures form the C5 nearest neighbor hydrogen-bond characteristic of extended structures, the Asn-containing molecule forms a doubly hydrogen-bonded bridge utilizing both the donor and the acceptor groups on the carboxamide side chain, while the Gln-containing structure only forms one side-chain−backbone hydrogen bond between the carboxamide C═O and the NHBn cap NH. In this case it appears that as a result of the more flexible Gln side chain in the extended backbone conformation *either* a side-chain-C-terminal C8 *or* a side-chain-N-terminal C9 hydrogen bond will be formed, while the less flexible Asn side chain readily accesses both types of stabilizing interactions. It may indeed seem counterintuitive that the more flexible Gln side chain is more limited in the formation of multiple side-chain−backbone hydrogen bonds than the less flexible Asn side chain, but in our previous work we found that there is an energy penalty of 1.22 kJ/mol in going from the C5//C8 in eQ to a C5//C9/C8 structure.[34]

As can be seen in Table 2, the L-chirality of the amino acids studied here results in χ_1 being similar in both extended structures (−137° in eN and −103° in eQ) with differences appearing in subsequent dihedrals. When viewed down the peptide backbone from the N→C termini, the functional groups jut out to the right side and then fold back over toward the backbone amide groups. The C5 hydrogen bonds appear within 8 cm^{-1} of one another, indicating similar hydrogen-bond strengths. Both the C8 and the C7 H bonds in eN occur with near-optimal distances and angles of approach: 2.23 Å/146° and 2.04 Å/160°, respectively. The AS C8 NH_2 stretch of eN is 52 cm^{-1} lower in frequency than the analogous eQ free stretch, which appears at 3562 cm^{-1}.

The C7 and analogous C8 NH stretch transitions in eN and eQ appear at 3279 and 3310 cm^{-1}, respectively. Given that the eQ C8 is ∼0.1 Å shorter than its C7 counterpart, it is natural to wonder why it appears 31 cm^{-1} higher in frequency. We note that the eN and eQ structures differ primarily in eN possessing a //C8/C7 bridged double-hydrogen-bonded structure while eQ forms only the C8 hydrogen bond. This suggests that cooperative hydrogen-bond strengthening could account for the discrepancy between the eN and the eQ C7 and C8 NH stretch frequencies, respectively. Indeed, eN is a triply hydrogen-bonded cycle, with all three hydrogen bonds experiencing cooperative effects, thereby increasing the NH bond distances and decreasing the NH stretch absorption frequencies. Since eQ lacks this hydrogen-bonded cycle, it would not experience the same magnitude of cooperative effects.

The peptide backbones in β-sheets adopt extended conformations which utilize the same C5 hydrogen bond found in eN and eQ. As pointed out in the Gln studies, this raises the intriguing possibility that the local extended conformation, supported by side-chain−backbone hydrogen bonds, could play a role in local β-strand formation on the way to β-sheet formation. As we have seen, however, neither Ac-

DOI: 10.1021/acs.jpca.8b08418
J. Phys. Chem. A 2018, 122, 8762−8775

Ala-Asn-NHBn nor Ac-Asn-Asn-NHBn adopts extended β-sheet structures in the gas phase. It would be interesting to see what intramolecular interactions dominate in even longer poly-Asn and poly-Gln peptides in the gas phase. In terms of free energy ranking, eN is second in energy, above γN (Table S2), raising the possibility that the local extended conformation could play a competitive role in a free energy environment. As mentioned above, the eN NHMe cap analogue is one of only two low-energy structures within 15 kJ/mol of global minimum, along with γN (Table S5).

4.3. Type I β-Turns. In both Ac-Ala-Asn-NHBn and Ac-Asn-Asn-NHBn, population is funneled into one conformational isomer: the type I β-turn. Given that both Ac-Asn-NHBn conformers incorporate bridged side-chain−backbone hydrogen bonds, it is curious that neither dipeptide includes such a bridged structure. Inspection of each assigned β-turn structure, however, yields a satisfying physical explanation. In order for the i+2 NH to engage in a strong C6 hydrogen bond with the i+2 carboxamide C═O while at the same time retaining the C10 hydrogen bond (that defines the β-turn), the i+2 Asn NH_2 group must be almost planar with the i+2 backbone C═O. This spatial relationship makes hydrogen bonding very unlikely.

It is important to note that both analogous Gln-containing dipeptides also exclusively form type I β-turns in the gas phase.[34,35] In what follows these four structures will be referred to as β_{AN}, β_{NN}, β_{AQ}, and β_{QQ}, where the subscripted letters abbreviate the amino acids in the dipeptide. We will use Figure 9 to guide the discussion, which presents and compares the structures and spectra of β_{AN} and β_{AQ} and β_{NN} and β_{QQ}. As the structures in Figure 9 and the dihedrals listed in Table 2 show, these four β-turns are quite similar to one another. Structural differences made manifest in the spectra do, however, exist, and it is to these details that we now turn.

The top half of Figure 9 displays the structures and spectra belonging to the C10//C6/π and C10//C7/π hydrogen-bonded conformers of β_{AN} and β_{AQ}, respectively. As one might expect, their hydride stretch spectra look very similar. The high-frequency stretch assigned to the π hydrogen-bound asymmetric NH_2 stretch is 18 cm^{-1} higher in frequency in β_{AQ} (3520 cm^{-1}) than in β_{AN} (3502 cm^{-1}). This is most likely a consequence of two factors: The NH_2 is more centered over the aromatic ring in β_{AN} than in β_{AQ}, and there is a weak interaction between the NH_2 group and the C-terminal C═O group. Indeed, in each pair of β-turn dipeptides the Asn and Gln residues utilize opposite NH groups for the $NH_2\cdots\pi$ interaction. The symmetric stretch pair occurs 107 and 112 cm^{-1} down in frequency from the asymmetric stretch in β_{AN} and β_{AQ}, respectively. The C-terminal asymmetric and symmetric stretch pairs in β_{NN} and β_{QQ} all appear within 3 cm^{-1} of their Ala-containing analogue stretches mentioned above, providing spectroscopic evidence that the C-terminal environment of the NH_2 groups are very similar within each residue pair. The free NH stretches in β_{AN} and β_{AQ} occur within 4 cm^{-1} of one another. The shorter and stronger C7 NH stretch fundamental is lower in frequency (1.97 Å, 3361 cm^{-1}) than the longer and weaker C6 NH stretch (2.08 Å, 3373 cm^{-1}). The β_{AN} and β_{AQ} C10 frequencies are within 10 cm^{-1} of one another, indicating similar hydrogen-bond strengths.

In going from Ac-A-N-NHBn to Ac-N-N-NHBn (and Gln analogues) the type I β-turn structure is preserved, with the N-terminal carboxamide group adding an additional C6 (C7) side-chain−backbone hydrogen bond (see Figure S6 for the overlap of the β_{AN} and β_{NN} backbones and Figure S7 for a direct comparison of their hydride stretch spectra). This conservation of structure is evident in Figure 9. The N-terminal free NH_2 AS and SS fundamentals appear at 3543/3430 and 3562/3444 cm^{-1} in β_{NN} and β_{QQ}, respectively. The shift to lower frequency in β_{NN} may again be attributed to a weak interaction between the N-terminal NH_2 and the amide C═O. It is heuristically pleasing to view the four highest frequency asymmetric NH_2 transitions between β_{NN} and β_{QQ} (Figure 9) as equivalent NH_2 groups in different environments. In order of decreasing frequency, we classify them in the following way: Free, Free with weak interaction, π hydrogen bond, π hydrogen bond with weak interaction, with each weak interaction resulting in an additional ∼20 cm^{-1} downshift in frequency.

The C10 hydrogen bonds in β_{NN} and β_{QQ} have NH stretch fundamentals within 5 cm^{-1} of one another, again indicating similar hydrogen-bond strength. Additionally, the interior C6 in β_{NN} and C7 in β_{QQ} are of similar strength, with transitions within 1 cm^{-1} of each other in the spectra. In contrast, the N-terminal C6 and C7 are separated from one another by 60 cm^{-1}. This can be understood in the context of hydrogen-bond distance: 2.16 Å in β_{NN} and a remarkably short 1.91 Å in β_{QQ} (see Figures S8 and S9 for the overlap of the β_{AN} and β_{AQ} and β_{NN} and β_{QQ}, respectively). The above spectroscopic and computational evidence suggests that glutamine is especially well setup to accommodate the β-turn via strong side-chain−backbone hydrogen-bond stabilization.

As with the shorter Asn-containing peptides, calculations were carried out on all structures within 30 kJ/mol of the global minimum to test the energetic influence of the NHBn cap, as well as to get an idea of the free energy landscape at room temperature. In the case of β_{AN}, substitution of NHBn for NHMe results in the C10//C7/π structure remaining on the global energy minimum (Table S6). β_{NN}, however, is displaced as the global energy minimum by a C10//C6/C7//**C11** structure (6.85 kJ/mol with NHBn cap) and takes up position as the second lowest energy structure (0.57 kJ/mol, Table S7, Figure S10). In this C10//C6/C7//**C11** structure the carboxamide NH_2 of the i+1 Asn residue engages in a H bond with the carboxamide C═O of the i+2 Asn residue, resulting in two large hydrogen-bonded cycles along the peptide backbone. In terms of free energy, both β_{AN} and β_{NN} retain their positions as the global energy minima (Tables S3 and S4). As with the shorter peptides discussed above, this indicates that the type I β-turns studied here are entropically competitive with other structures even at room temperature.

Upon cooling in a supersonic expansion, the entirety of the population of both β_{AN} and β_{NN} is funneled into a type I β-turn that is stabilized by the Asn side chains. The robustness of these structures to temperature and type of cap is in keeping with the prevalence of Asn-containing β-turns in biological environments.[61,62] To get an idea of the similarity in turn parameters between these gas-phase structures and those in naturally occurring biologically relevant molecules, we compare the calculated backbone φ and ψ dihedral angles of β_{AN} and β_{NN} with those found in the Protein Data Bank comprised of the following four generic amino acid residue order: X(AN)X for β_{AN} and X(NN)X for β_{NN} (Table 2 and Tables S8 and S9). We find that, in both cases, the calculated gas-phase parameters are in good agreement with both the crystal structure average values as well as the canonical literature

DOI: 10.1021/acs.jpca.8b08418
J. Phys. Chem. A 2018, 122, 8762−8775

values,[58] indicating that the gas-phase structures characterized in this work are fundamentally preserved and preferred in the condensed phase. Indeed, a recent study by Mons et al. also found the type I β-turn to be among the observed conformations in gas-phase studies of Ac-Phe-Asn-NH_2. Through a Protein Data Bank search they observed that with Asn in the i+2 position of the β-turn it is not uncommon for water molecules to bridge the i+2 amide NH and side-chain C═O, the two groups involved in the C6 hydrogen bond. They proposed that in hydrophilic environments this water-bridged structure could orient and stabilize the local protein backbone in such a way that promotes β-turn formation. This proposition is especially enticing in light of the regularity with which Asn appears in the i+2 position of native protein β-turns.[61,62]

5. CONCLUSIONS

In this study we determined the inherent folding preferences of three Asn-containing, capped peptides: Ac-Asn-NHBn, Ac-Ala-Asn-NHBn, and Ac-Asn-Asn-NHBn. Using conformation-specific infrared and ultraviolet spectroscopy we found that Ac-Asn-NHBn takes both an inverse γ-turn ($C7_{eq}$) and a tentatively assigned extended conformation (C5), while both capped dipeptides Ac-Ala-Asn-NHBn and Ac-Asn-Asn-NHBn have all of their population funneled into a type I β-turn. These two turn types and extended structure appear regularly within the secondary structural framework of nature. In each case, a single backbone−backbone hydrogen bond is supported by at least one side-chain−backbone stabilizing interaction.

In γN, an unusually strong $C7_{eq}$ hydrogen bond forms the inverse turn, with a doubly hydrogen-bonded //C6/C7-bridged side-chain−backbone motif resulting in a triamide H-bonded cycle that appears to be cooperatively strengthened. The analogous Gln-containing peptide also forms the same cooperatively strengthened bridged side-chain−backbone-supported inverse γ-turn. The extended backbone of eN is supported by a //C8/C7-bridged side-chain−backbone double hydrogen bond, an auxiliary interaction not accessible to Gln as a direct result of its more flexible side chain. The C10-containing type I β-turn structures of β_{AN} and β_{NN} are further stabilized by side-chain−backbone C6 H bonds between the Asn NH_2 and the C═O group on its peptide residue. These β-turns are closely similar to those found in protein crystals, where the relevant Ala and/or Asn residues occupy the i+1 and i+2 positions of the turn. They are also close in form to the analogous β_{AQ} and β_{QQ} turns, as characterized by the backbone φ and ψ dihedral angles. Spectroscopic and computational evidence of strong side-chain−backbone hydrogen bonding suggest that glutamine is especially well set up for β-turn accommodation.

In the case of all Asn-containing peptides studied here, energy optimizations performed with the NHMe-capped analogues predicted that the lowest energy conformations observed with the NHBn cap remain either the lowest or, in the case of β_{AN}, the second lowest energy conformation when the phenyl ring is removed. Additionally, the ranking of the conformations in free energy at room temperature confirmed that the assigned structures occupy the most stable, global free energy minimum positions as well. These results provide evidence that the assigned structures will have significant population over a wide range of conditions. Furthermore, the three structural motifs (inverse γ-turn, extended, type I β-turn) that are stabilized by Asn are all prevalent to some degree in nature.

The fundamental similarity of these Asn- and Gln-containing peptides is especially interesting in light of the requirement for specific amino acid type, rather than sequence, in prion formation, as well as the similar fibrillar properties that polyasparagine exhibits with respect to polyglutamine.[10,63,64] These initial conformational tests of asparagine's local conformational preferences at the dipeptide length would benefit greatly from extension to peptides containing longer sequences of Asn, Gln, and combinations thereof, with the goal of determining the effect that increasing peptide length has on their inherent structural preferences.

■ ASSOCIATED CONTENT

Supporting Information

The Supporting Information is available free of charge on the ACS Publications website at DOI: 10.1021/acs.jpca.8b08418.

Synthetic procedure for Ac-Asn-NHBn, Ac-Ala-Asn-NHBn, Ac-Asn-Asn-NHBn, R2PI, and IR−UV hole-burning spectra of Ac-Asn-NHBn, Ac-Ala-Asn-NHBn, and Ac-Asn-Asn-NHBn, relaxed benzyl potential energy scan of Ac-Asn-NHBn conf A, structural comparison of conf A and conf A^{Rot}, hydrogen-bonding cycle parameters for Asn, Gln, and β-amino acid-containing peptides, backbone overlap and hydride stretch comparison spectra of Ac-Ala-Asn-NHBn and Ac-Asn-Asn-NHBn, backbone overlap of Ac-Ala-Asn-NHBn and Ac-Ala-Gln-NHBn and Ac-Asn-Asn-NHBn and Ac-Gln-Gln-NHBn, free energy corrections, energy reordering upon NHBn substitution for NHMe cap, comparison of NHBn and NHMe-capped Ac-Asn-Asn-NHBn conf A with calculated low-energy C10//C6/C7//**C11** structure, comparison of type I β-turn dihedral angles (PDF)

■ AUTHOR INFORMATION

Corresponding Author

*E-mail: zwier@purdue.edu. Phone: (765) 494-5278.

ORCID

Karl N. Blodgett: 0000-0002-6827-0328
Soo Hyuk Choi: 0000-0003-4066-6504
Timothy S. Zwier: 0000-0002-4468-5748

Notes

The authors declare no competing financial interest.

■ ACKNOWLEDGMENTS

The Purdue authors gratefully acknowledge support for this research from the National Science Foundation (NSF Grant CHE-1456256 and CHE-1764148). J.L. and S.H.C. acknowledge support from the National Research Foundation of Korea (NRF-2016R1A2B4012798).

■ REFERENCES

(1) Zhang, Y.; Man, V. H.; Roland, C.; Sagui, C. Amyloid Properties of Asparagine and Glutamine in Prion-Like Proteins. *ACS Chem. Neurosci.* **2016**, *7* (5), 576−587.

(2) Perutz, M. F.; Pope, B. J.; Owen, D.; Wanker, E. E.; Scherzinger, E. Aggregation of Proteins with Expanded Glutamine and Alanine Repeats of the Glutamine-Rich and Asparagine-Rich Domains of Sup35 and of the Amyloid B-Peptide of Amyloid Plaques. *Proc. Natl. Acad. Sci. U. S. A.* **2002**, *99* (8), 5596−5600.

DOI: 10.1021/acs.jpca.8b08418
J. Phys. Chem. A 2018, 122, 8762−8775

(3) Michelitsch, M. D.; Weissman, J. S. A Census of Glutamine/Asparagine-Rich Regions: Implications for Their Conserved Function and the Prediction of Novel Prions. *Proc. Natl. Acad. Sci. U. S. A.* **2000**, *97* (22), 11910−11915.
(4) Okazawa, H. Glutamine/Asparagine-Rich Regions in Proteins and Polyglutamine Diseases. In *Protein Misfolding, Aggregation, and Conformational Diseases: Part B: Molecular Mechanisms of Conformational Diseases*; Uversky, V. N., Fink, A. L., Eds.; Springer US: Boston, MA, 2007; pp 451−463.
(5) Hoffner, G.; Djian, P. Polyglutamine Aggregation in Huntington Disease: Does Structure Determine Toxicity? *Mol. Neurobiol.* **2015**, *52* (3), 1297−1314.
(6) Wolfe, K. J.; Cyr, D. M. Amyloid in Neurodegenerative Diseases: Friend or Foe? *Semin. Cell Dev. Biol.* **2011**, *22* (5), 476−481.
(7) Chiti, F.; Dobson, C. M. Protein Misfolding, Functional Amyloid, and Human Disease. *Annu. Rev. Biochem.* **2006**, *75*, 333−366.
(8) Ross, C. A. Polyglutamine Pathogenesis: Emergence of Unifying Mechanisms for Huntington's Disease and Related Disorders. *Neuron* **2002**, *35* (5), 819−822.
(9) Mangiarini, L.; Sathasivam, K.; Seller, M.; Cozens, B.; Harper, A.; Hetherington, C.; Lawton, M.; Trottier, Y.; Lehrach, H.; Davies, S. W. Exon 1 of the Hd Gene with an Expanded Cag Repeat Is Sufficient to Cause a Progressive Neurological Phenotype in Transgenic Mice. *Cell* **1996**, *87* (3), 493−506.
(10) Peters, T. W.; Huang, M. Protein Aggregation and Polyasparagine-Mediated Cellular Toxicity in Saccharomyces Cerevisiae. *Prion* **2007**, *1* (2), 144−153.
(11) Fornai, F.; Ferrucci, M.; Gesi, M.; Di Poggio, A. B.; Giorgi, F.; Biagioni, F.; Paparelli, A. A Hypothesis on Prion Disorders: Are Infectious, Inherited, and Sporadic Causes So Distinct? *Brain Res. Bull.* **2006**, *69* (2), 95−100.
(12) Halfmann, R.; Alberti, S.; Krishnan, R.; Lyle, N.; O'Donnell, C. W.; King, O. D.; Berger, B.; Pappu, R. V.; Lindquist, S. Opposing Effects of Glutamine and Asparagine Govern Prion Formation by Intrinsically Disordered Proteins. *Mol. Cell* **2011**, *43* (1), 72−84.
(13) An, L.; Harrison, P. M. The Evolutionary Scope and Neurological Disease Linkage of Yeast-Prion-Like Proteins in Humans. *Biol. Direct* **2016**, *11* (1), 32.
(14) Kurt, T. D.; Aguilar-Calvo, P.; Jiang, L.; Rodriguez, J. A.; Alderson, N.; Eisenberg, D. S.; Sigurdson, C. J. Asparagine and Glutamine Ladders Promote Cross-Species Prion Conversion. *J. Biol. Chem.* **2017**, *292* (46), 19076−19086.
(15) Geschwind, M. D. Prion Diseases. *CONTINUUM: Lifelong Learning in Neurology* **2015**, *21*, 1612−1638.
(16) Prusiner, S. B.; Barry, R. A.; McKinley, M. P.; Bellinger, C. G.; Meyer, R. K.; DeArmond, S. J.; Kingsbury, D. T. Prion Diseases. In *Viruses, Immunity, and Mental Disorders*; Springer, 1987; pp 23−32.
(17) Sawaya, M. R.; Sambashivan, S.; Nelson, R.; Ivanova, M. I.; Sievers, S. A.; Apostol, M. I.; Thompson, M. J.; Balbirnie, M.; Wiltzius, J. J.; McFarlane, H. T. Atomic Structures of Amyloid Cross-B Spines Reveal Varied Steric Zippers. *Nature* **2007**, *447* (7143), 453.
(18) Nelson, R.; Sawaya, M. R.; Balbirnie, M.; Madsen, A. Ø.; Riekel, C.; Grothe, R.; Eisenberg, D. Structure of the Cross-B Spine of Amyloid-Like Fibrils. *Nature* **2005**, *435* (7043), 773−778.
(19) Benzinger, T. L.; Gregory, D. M.; Burkoth, T. S.; Miller-Auer, H.; Lynn, D. G.; Botto, R. E.; Meredith, S. C. Propagating Structure of Alzheimer's B-Amyloid (10−35) Is Parallel B-Sheet with Residues in Exact Register. *Proc. Natl. Acad. Sci. U. S. A.* **1998**, *95* (23), 13407−13412.
(20) Paravastu, A. K.; Leapman, R. D.; Yau, W.-M.; Tycko, R. Molecular Structural Basis for Polymorphism in Alzheimer's B-Amyloid Fibrils. *Proc. Natl. Acad. Sci. U. S. A.* **2008**, *105* (47), 18349−18354.
(21) Petkova, A. T.; Yau, W.-M.; Tycko, R. Experimental Constraints on Quaternary Structure in Alzheimer's B-Amyloid Fibrils. *Biochemistry* **2006**, *45* (2), 498−512.
(22) Shewmaker, F.; Wickner, R. B.; Tycko, R. Amyloid of the Prion Domain of Sup35p Has an in-Register Parallel B-Sheet Structure. *Proc. Natl. Acad. Sci. U. S. A.* **2006**, *103* (52), 19754−19759.
(23) Gorkovskiy, A.; Thurber, K. R.; Tycko, R.; Wickner, R. B. Locating Folds of the in-Register Parallel B-Sheet of the Sup35p Prion Domain Infectious Amyloid. *Proc. Natl. Acad. Sci. U. S. A.* **2014**, *111* (43), E4615−E4622.
(24) Kryndushkin, D. S.; Wickner, R. B.; Tycko, R. The Core of Ure2p Prion Fibrils Is Formed by the N-Terminal Segment in a Parallel Cross-B Structure: Evidence from Solid-State Nmr. *J. Mol. Biol.* **2011**, *409* (2), 263−277.
(25) Ngo, S.; Gu, L.; Guo, Z. Hierarchical Organization in the Amyloid Core of Yeast Prion Protein Ure2. *J. Biol. Chem.* **2011**, *286* (34), 29691−29699.
(26) Baxa, U.; Wickner, R. B.; Steven, A. C.; Anderson, D. E.; Marekov, L. N.; Yau, W.-M.; Tycko, R. Characterization of B-Sheet Structure in Ure2p1−89 Yeast Prion Fibrils by Solid-State Nuclear Magnetic Resonance. *Biochemistry* **2007**, *46* (45), 13149−13162.
(27) DePace, A. H.; Santoso, A.; Hillner, P.; Weissman, J. S. A Critical Role for Amino-Terminal Glutamine/Asparagine Repeats in the Formation and Propagation of a Yeast Prion. *Cell* **1998**, *93* (7), 1241−1252.
(28) Fiumara, F.; Fioriti, L.; Kandel, E. R.; Hendrickson, W. A. Essential Role of Coiled Coils for Aggregation and Activity of Q/N-Rich Prions and Polyq Proteins. *Cell* **2010**, *143* (7), 1121−1135.
(29) Lu, X.; Murphy, R. M. Asparagine Repeat Peptides: Aggregation Kinetics and Comparison with Glutamine Repeats. *Biochemistry* **2015**, *54* (31), 4784−4794.
(30) Paul, K. R.; Ross, E. D. Controlling the Prion Propensity of Glutamine/Asparagine-Rich Proteins. *Prion* **2015**, *9* (5), 347−354.
(31) Vasudev, P. G.; Banerjee, M.; Ramakrishnan, C.; Balaram, P. Asparagine and Glutamine Differ in Their Propensities to Form Specific Side Chain-Backbone Hydrogen Bonded Motifs in Proteins. *Proteins: Struct., Funct., Genet.* **2012**, *80* (4), 991−1002.
(32) Alemán, C.; Puiggalí, J. Conformational Preferences of the Asparagine Residue. Gas-Phase, Aqueous Solution, and Chloroform Solution Calculations on the Model Dipeptide. *J. Phys. Chem. B* **1997**, *101* (17), 3441−3446.
(33) Habka, S.; Sohn, W. Y.; Vaquero-Vara, V.; Geleoc, M.; Tardivel, B.; Brenner, V.; Gloaguen, E.; Mons, M. On the Turn-Inducing Properties of Asparagine: The Structuring Role of the Amide Side Chain, from Isolated Model Peptides to Crystallized Proteins. *Phys. Chem. Chem. Phys.* **2018**, *20*, 3411.
(34) Walsh, P. S.; Dean, J. C.; McBurney, C.; Kang, H.; Gellman, S. H.; Zwier, T. S. Conformation-Specific Spectroscopy of Capped Glutamine-Containing Peptides: Role of a Single Glutamine Residue on Peptide Backbone Preferences. *Phys. Chem. Chem. Phys.* **2016**, *18* (16), 11306−11322.
(35) Walsh, P. S.; Blodgett, K. N.; McBurney, C.; Gellman, S. H.; Zwier, T. S. Inherent Conformational Preferences of Ac-Gln-Gln-Nhbn: Sidechain Hydrogen Bonding Supports a B-Turn in the Gas Phase. *Angew. Chem., Int. Ed.* **2016**, *55* (47), 14618−14622.
(36) James, W. H.; Baquero, E. E.; Choi, S. H.; Gellman, S. H.; Zwier, T. S. Laser Spectroscopy of Conformationally Constrained A/B-Peptides: Ac-Acpc-Phe-Nhme and Ac-Phe-Acpc-Nhme. *J. Phys. Chem. A* **2010**, *114* (3), 1581−1591.
(37) Baquero, E. E.; James, W. H.; Choi, S. H.; Gellman, S. H.; Zwier, T. S. Single-Conformation Ultraviolet and Infrared Spectroscopy of Model Synthetic Foldamers: B-Peptides Ac-B3-Hphe-Nhme and Ac-B3-Htyr-Nhme. *J. Am. Chem. Soc.* **2008**, *130* (14), 4784−4794.
(38) James, W. H.; Baquero, E. E.; Shubert, V. A.; Choi, S. H.; Gellman, S. H.; Zwier, T. S. Single-Conformation and Diastereomer Specific Ultraviolet and Infrared Spectroscopy of Model Synthetic Foldamers: A/B-Peptides. *J. Am. Chem. Soc.* **2009**, *131* (18), 6574−6590.
(39) Baquero, E. E.; James, W. H.; Choi, S. H.; Gellman, S. H.; Zwier, T. S. Single-Conformation Ultraviolet and Infrared Spectroscopy of Model Synthetic Foldamers: B-Peptides Ac-B3-Hphe-B3-

DOI: 10.1021/acs.jpca.8b08418
J. Phys. Chem. A 2018, 122, 8762−8775

Hala-Nhme and Ac-B3-Hala-B3-Hphe-Nhme. *J. Am. Chem. Soc.* **2008**, *130* (14), 4795−4807.
(40) Gord, J. R.; Walsh, P. S.; Fisher, B. F.; Gellman, S. H.; Zwier, T. S. Mimicking the First Turn of an A-Helix with an Unnatural Backbone: Conformation-Specific Ir and Uv Spectroscopy of Cyclically Constrained B/Γ-Peptides. *J. Phys. Chem. B* **2014**, *118* (28), 8246−8256.
(41) Lubman, D. M. Analytical Multiphoton Ionization Mass Spectrometry. Part Ii. Applications. *Mass Spectrom. Rev.* **1988**, *7* (6), 559−592.
(42) Dean, J. C.; Buchanan, E. G.; Zwier, T. S. Mixed 14/16 Helices in the Gas Phase: Conformation-Specific Spectroscopy of Z-(Gly)N, N = 1, 3, 5. *J. Am. Chem. Soc.* **2012**, *134* (41), 17186−17201.
(43) Dean, J. C.; Kusaka, R.; Walsh, P. S.; Allais, F.; Zwier, T. S. Plant Sunscreens in the Uv-B: Ultraviolet Spectroscopy of Jet-Cooled Sinapoyl Malate, Sinapic Acid, and Sinapate Ester Derivatives. *J. Am. Chem. Soc.* **2014**, *136* (42), 14780−14795.
(44) Frisch, M. J.; Trucks, G. W.; Schlegel, H. B.; Scuseria, G. E.; Robb, M. A.; Cheeseman, J. R.; Scalmani, G.; Barone, V.; Mennucci, B.; Petersson, G. A.; et al. *Gaussian 09*; Gausian, Inc.: Wallingford, CT, 2010.
(45) Grimme, S. Accurate Description of Van Der Waals Complexes by Density Functional Theory Including Empirical Corrections. *J. Comput. Chem.* **2004**, *25* (12), 1463−1473.
(46) Grimme, S. Semiempirical Hybrid Density Functional with Perturbative Second-Order Correlation. *J. Chem. Phys.* **2006**, *124* (3), 034108.
(47) Berman, H. M.; Westbrook, J.; Feng, Z.; Gilliland, G.; Bhat, T. N.; Weissig, H.; Shindyalov, I. N.; Bourne, P. E. The Protein Data Bank. *Nucleic Acids Res.* **2000**, *28* (1), 235−242.
(48) Leader, D. P.; Milner-White, E. J. Motivated Proteins: A Web Application for Studying Small Three-Dimensional Protein Motifs. *BMC Bioinf.* **2009**, *10* (1), 60.
(49) Nakanaga, T.; Ito, F. Investigations on the Hydrogen Bond Interaction in the Aniline−Furan Complex and Its Cation by Infrared Depletion Spectroscopy. *J. Phys. Chem. A* **1999**, *103* (28), 5440−5445.
(50) Buchanan, E. G.; James, W. H.; Choi, S. H.; Guo, L.; Gellman, S. H.; Müller, C. W.; Zwier, T. S. Single-Conformation Infrared Spectra of Model Peptides in the Amide I and Amide Ii Regions: Experiment-Based Determination of Local Mode Frequencies and Inter-Mode Coupling. *J. Chem. Phys.* **2012**, *137* (9), 094301.
(51) Torii, H. Mechanism of the Secondary Structure Dependence of the Infrared Intensity of the Amide Ii Mode of Peptide Chains. *J. Phys. Chem. Lett.* **2012**, *3* (1), 112−116.
(52) Torii, H.; Kawanaka, M. Secondary Structure Dependence and Hydration Effect of the Infrared Intensity of the Amide Ii Mode of Peptide Chains. *J. Phys. Chem. B* **2016**, *120* (8), 1624−1634.
(53) Maechling, C. R.; Clemett, S. J.; Engelke, F.; Zare, R. N. Evidence for Thermalization of Surface-Desorbed Molecules at Heating Rates of 108 K/S. *J. Chem. Phys.* **1996**, *104* (21), 8768−8776.
(54) Handschuh, M.; Nettesheim, S.; Zenobi, R. Is Laser Heating Advantageous for Thermal Desorption of Large Polar Molecules? *J. Chem. Phys.* **1997**, *107* (7), 2603−2610.
(55) Brenner, V.; Piuzzi, F.; Dimicoli, I.; Tardivel, B.; Mons, M. Spectroscopic Evidence for the Formation of Helical Structures in Gas-Phase Short Peptide Chains. *J. Phys. Chem. A* **2007**, *111* (31), 7347−7354.
(56) Loquais, Y.; Gloaguen, E.; Habka, S.; Vaquero-Vara, V.; Brenner, V.; Tardivel, B.; Mons, M. Secondary Structures in Phe-Containing Isolated Dipeptide Chains: Laser Spectroscopy Vs Quantum Chemistry. *J. Phys. Chem. A* **2015**, *119* (23), 5932−5941.
(57) Milner-White, E. J. Situations of Gamma-Turns in Proteins: Their Relation to Alpha-Helices, Beta-Sheets and Ligand Binding Sites. *J. Mol. Biol.* **1990**, *216* (2), 385−397.
(58) Lewis, P. N.; Momany, F. A.; Scheraga, H. A. Chain Reversals in Proteins. *Biochim. Biophys. Acta, Protein Struct.* **1973**, *303* (2), 211−229.
(59) Chin, W.; Mons, M.; Dognon, J.-P.; Piuzzi, F.; Tardivel, B.; Dimicoli, I. Competition between Local Conformational Preferences and Secondary Structures in Gas-Phase Model Tripeptides as Revealed by Laser Spectroscopy and Theoretical Chemistry. *Phys. Chem. Chem. Phys.* **2004**, *6* (10), 2700−2709.
(60) Chin, W.; Piuzzi, F.; Dimicoli, I.; Mons, M. Probing the Competition between Secondary Structures and Local Preferences in Gas Phase Isolated Peptide Backbones. *Phys. Chem. Chem. Phys.* **2006**, *8* (9), 1033−1048.
(61) Hutchinson, E. G.; Thornton, J. M. A Revised Set of Potentials for B-Turn Formation in Proteins. *Protein Sci.* **1994**, *3* (12), 2207−2216.
(62) Chou, P. Y.; Fasman, G. D. Prediction of Beta-Turns. *Biophys. J.* **1979**, *26* (3), 367−373.
(63) Ross, E. D.; Baxa, U.; Wickner, R. B. Scrambled Prion Domains Form Prions and Amyloid. *Mol. Cell. Biol.* **2004**, *24* (16), 7206−7213.
(64) Ross, E. D.; Edskes, H. K.; Terry, M. J.; Wickner, R. B. Primary Sequence Independence for Prion Formation. *Proc. Natl. Acad. Sci. U. S. A.* **2005**, *102* (36), 12825−12830.

DOI: 10.1021/acs.jpca.8b08418
J. Phys. Chem. A 2018, 122, 8762−8775